

Remote Long Period Gratings/Fiber Bragg Gratings sensor based on Raman amplification

Thiago V. N. Coelho, A. Guerreiro, Pedro A. S. Jorge and M. J. Pontes

Abstract— In this work, we analyze a remote optical sensor system composed of two Fiber Bragg Gratings (FBGs) and one Long Period Grating (LPG) capable of simultaneously sensing the temperature and the refractive index, separated by 50 km from the optical source and the interrogation unit. Since the active components of the system and the sensor head are separated over such a large distance, it is necessary to consider Raman amplification to strengthen the optical signal. We present both experimental measurements and the results of numerical simulations, which describe the signal evolution and predict the measurement results for a remote sensor based on a LPG. The simulation codes are also used to study a hybrid sensor composed of two FBGs with a LPG. We show that the power ratio between the two central wavelengths of the FBG has a linear relation with the change of refractive index of the sensed medium.

Index Terms— Optical Sensor, Fiber Bragg Gratings, Long Period Gratings, Raman Amplification

I. INTRODUCTION

Fiber Bragg Gratings (FBGs) and Long Period Gratings (LPGs) are optical in fiber devices widely used for monitoring several environmental parameters (including pressure, temperature, refractive index, etc.), which can be used in places polluted by electromagnetic radiation, in situations with difficult access and for monitoring structural health, thanks to their small size and facility to be incorporated into the optical network systems [1]. For these sensor schemes to monitor areas placed so far away from the monitoring unit, it is necessary to consider optical amplification, which can affect the quality of the optical signal and decrease the sensitivity of the monitoring systems.

Erbium Doped Fiber Amplifiers (EDFAs) and Raman Amplification are the most mature and available technologies to amplify the optical signal. Unlike EDFA, which needs a special fiber (an erbium doped fiber) to amplify the signal and has a limited amplification bandwidth, Raman amplifiers use standard fibers and have a gain bandwidth which can be adjusted by adequately choosing the number, power and

central wavelength of the pumps. This promotes Raman Amplification as the best amplification technology for remote sensing.

In this paper, we present a numerical model that describes the propagation and interactions of the pumps and the sensor signal along the fiber. This model is validated by the comparison of the experimental and simulation results applied on the LPG sensor. This model was also used to simulate a Hybrid sensor configuration. The first section describes the numerical method used to represent the propagation behavior of the signals and pumps in the Raman Amplifiers System. In the section two, we discussed the methodologies used in this work, explaining the modifications made on the simulation model introduced by Coelho et al. [2] for the case of remote sensing. The third section presents the experimental and simulation results and section four presents the conclusion of this work.

II. NUMERICAL MODEL BASED ON RAMAN INTERACTIONS

Raman amplifiers are based on the nonlinear effect of Stimulated Raman Scattering (SRS). Its main characteristic is the energy transfer from one or more pump wavelengths to the wavelength signals [3].

A numerical model [2,4] was used to describe the interaction between the signal and pump propagation in the fiber taking into account Raman Amplification effects, the single and double Rayleigh scattering, the amplifying spontaneous emission (ASE) noise, polarization effects and the interaction between signal and pumps, signal-signal and pump-pump. The main equation is (1):

$$\begin{aligned}
 \frac{dP_v^\pm}{dz} &= \mp \alpha_v P_v^\pm \pm \epsilon_v P_v^\mp \\
 \pm P_v^\pm &\sum_{\mu > \nu} \frac{C_{R\mu\nu}}{\Gamma} (P_\mu^+ + P_\mu^-) \\
 \pm 2\hbar\nu B_e &\sum_{\mu > \nu} \frac{C_{R\mu\nu}}{\Gamma} (P_\mu^+ + P_\mu^-) [1 + \eta(T)] \\
 \mp P_v^\pm &\sum_{\mu < \nu} \frac{\omega_\nu C_{R\nu\mu}}{\omega_\mu \Gamma} (P_\mu^+ + P_\mu^-) \\
 \mp P_v^\pm &\sum_{\mu < \nu} \frac{\omega_\nu C_{R\nu\mu}}{\omega_\mu \Gamma} [1 + \eta(T)] 4\hbar\mu B_e
 \end{aligned} \tag{1}$$

Manuscript received June 20, 2011. This work was supported in part by CAPES (Coordenação de Aperfeiçoamento de Pessoal de Nível Superior) and FAPES (Fundação de Amparo a Pesquisa do Espírito Santo).

Thiago V. N. Coelho is with the INESC Porto, Porto, CO 4150-179 Portugal. Pphone: 351 220 402 301; fax: 351 220 402 437; e-mail: tncoelho@inescporto.pt).

A. Guerreiro and Pedro A. S. Jorge are with the INESC Porto, Porto, CO 4150-179 Portugal e-mail: arieltguerreiro@ gmail.com, pedro.jorge@fc.up.pt).

M. J. Pontes is with the Electrical Engineering Department, Universidade Federal do Espírito Santo, Vitória/ES, CO 29060-900 Brazil, (e-mail: mjpontes@ele.ufes.br).

where P_μ , P_ν , α_μ e α_ν are the powers and attenuation coefficients of the frequencies μ and ν respectively, the superscripts + and - indicate the forward and backward propagation in the z axis direction, $C_{R\mu\nu}$ is the Raman gain efficiency between the frequencies μ and ν , Γ is the polarization factor and takes as a value 1 if the polarizations are preserved and two case the polarizations are not maintained, ϵ_ν is the Rayleigh scattering coefficient and B_e is noise bandwidth considered.

III. METHODOLOGY

The propagation equations (1) for the source, signal and the pumps was solved using the MatLab® BVP packet and imposing the necessary boundary conditions using known values of the signal in some positions along the fiber. In the simulations, the source signal is propagated along the fiber until it reaches the sensor at the end of the fiber and reflects back the signal to be measured. To validate the model, we consider a LPG sensor and compared the results of the simulation with the experimental measurements obtained using the setup described in Fig. 1.

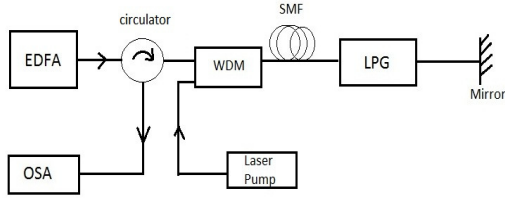


Figure 1. LPG remote sensor setup with Raman amplification applied in the LPG signal

The signal used was a broadband ASE source and the pump laser is a stable coherent high power source with wavelength centered in 1450 nm. The resonance wavelength of the LPG is near 1545 nm, the optical fiber used was the SMF 28 Corning and the mirror has 50% reflectivity in the entire spectral bandwidth of the ASE source. The Fig. 2 shows the spectral source measured at the reflected sensor output.

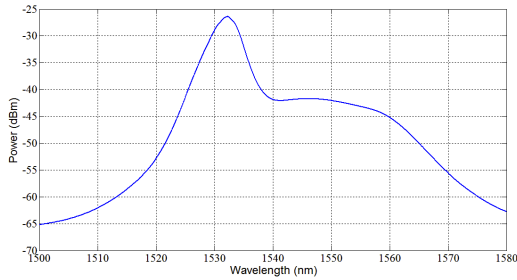


Figure 2. ASE broadband source

The boundary conditions used for the sensor system are similar but not exactly equal to those considered in telecommunications systems. Like in the later, it is considered that there are four light sources injected in the fiber: a forward signal and a forward pump or pumps, which are injected in the beginning of the fiber, and a backward signal and backward pump, which are injected at the end of the fiber, as depicted in

Fig. 3.

However, unlike the telecommunications systems where the backward signal and pump are usually null, in the case of the sensor the backward signal results from the transmitted forward signal as it is reflected in the sensor head. Since there is a detuning between the forward pump and the reflection wavelength of the sensor head, it is possible to neglect the reflected pump signal and consider the backward pump as null.

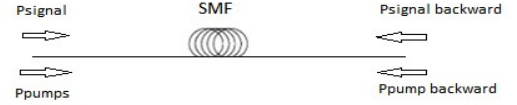
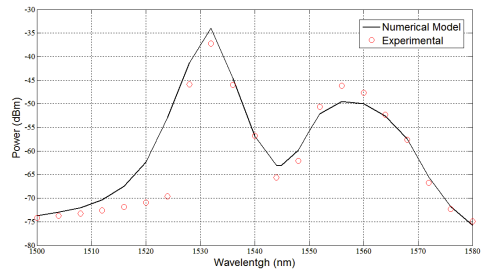


Figure 3. Boundary conditions applied in the numerical solution.

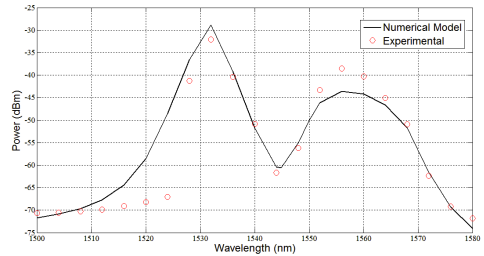
Unfortunately, it is impossible to know a priori the backward signal without having computed the transmission of the forward signal and pumps along the fiber. To overcome this difficulty, we applied the numerical solution in three steps: i) First we assume that both the backward signal and pump are null and propagate the forward signal and pump along the fiber using values identical to the experimental setup. ii) Then, using the reflection characteristics of the sensor head, we compute the reflected signal. iii) Finally, we repeat the first step but consider that the backward signal is identical to the value obtained in the step ii). This code was used to simulate not only a simple sensor head with just a LPG, which was used to validate the code, but also the hybrid sensor consisting of two FBGs and one LPG for different environmental refractive indexes.

IV. RESULTS

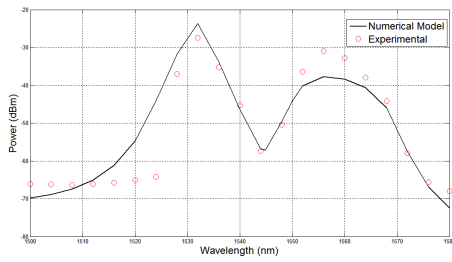
In Fig. 4 it is shown the experimental and simulation results for the setup shown in Fig. 1 used to validate the numerical method, where the sensor head consists only of an LPG. The fiber used is a 50 km Corning SMF 28 and the power of the pump laser varies from 600 mW to 1W.



(a)



(b)



(c)

Figure 4 – The experimental and simulation results for the setup in Figure 2 using a laser pump with (a) 600 mW, (b) 800 mW e (c) 1000 mW.

The results shown in Fig. 4 demonstrate that the numerical simulations can effectively reproduce the main features observed in the experiment. The main differences occur for lower wavelengths in the spectrum where the simulations predict a higher power than is measured in the experiment. This can be accounted by the small number of sampling points of the spectrum used in the simulations which results in an underestimation of the transference of power from the low to the high wavelengths.

After validating the numerical method, the same method was applied to the hybrid sensor [5] shown in Fig. 5 to study the impact of measure of the index refraction.

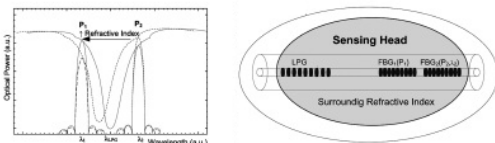


Figure 5 – Hybrid optical sensor based on LPG and FBGs [4]

Fig. 6 shows the relation of the power ratio (parameter R), which is the power ratio between the FBGs at the receiver, and the refractive index changes obtained from the simulations. The FBGs are centered around 1535.5 nm and 1546.5 nm, the LPG resonance wavelength is 1542.5 nm with a bandwidth of 15 nm. A flat optical broadband source with -30dBm optical power per channel was considered and two power pumps with 350 mW at 1441.8 and 1444 nm were used to provide a better profile of the gain spectrum.

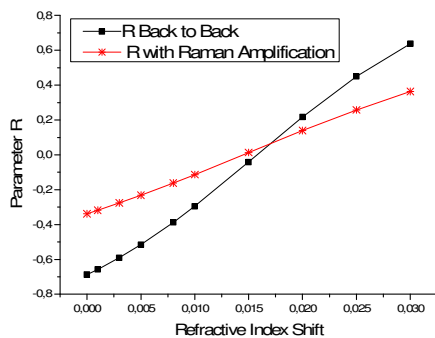


Figure 6 – R parameter vs. Refractive index shift for the back to back and Raman Amplification case

In Fig. 6, we compare the sensitivity of the parameter R with the change of refractive index between a back to back configuration, where the sensor head is connected directly to the interrogation unit (and therefore without amplification) and the remote configuration, where the signal must propagate back along the fiber (and therefore requires amplification). The results show that amplification degrades the sensor sensitivity. An explanation is that in the remote configuration the same optical fiber is used for return channel and for signal amplification. Consequently, the signal is polluted by the ASE noise and the Rayleigh scattering, yielding a degradation of the quality of OSNR ratio. Another problem with this remote configuration is the inefficiency of the amplification since much power of the pumps is used to amplify wavelengths that are rejected by the sensor head and are not represented in the reflected signal.

A simple way to overcome these difficulties is to use two different fibers and separate the channel which connects the source of the signal and the sensor head from the channel of amplification and return of the signal. This reduces both the ASE noise and backward Rayleigh scattering in the return fiber. Other alternative is to use a power splitter and perform amplification in both fibers. So the setup described in the Fig. 7 are used prove the concept.

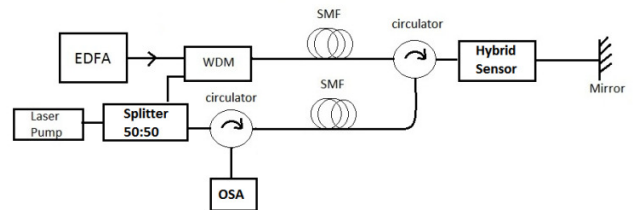


Figure 7. Hybrid remote sensor setup with Raman amplification applied in the both channels

In the Fig. 8 shows the responses of the first setup and the modification proposal in the Fig. 7 to add a return channel.

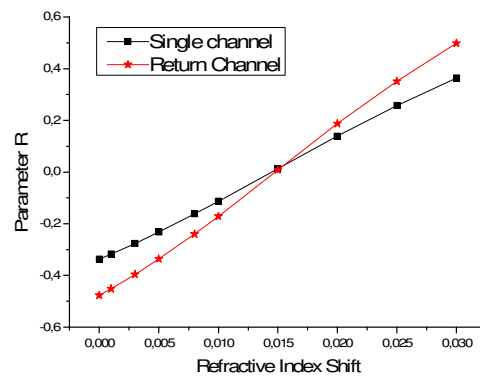


Figure 8 – R parameter vs. Refractive index shift for the single channel setup and the setup with return channel

Analyzing the response showed by Fig. 8 is obviously that the return channel setup exhibits an improvement into the sensibility of the sensor system, this better response is due to elimination by the return channel of the noise generated by the

Rayleigh Scattering of broadband source and the ASE from the first channel, causing a improvement in the OSNR level in the return channel as can be seen in the Fig. 9 that shows the relation between the OSNR level and SMF length by the both systems.

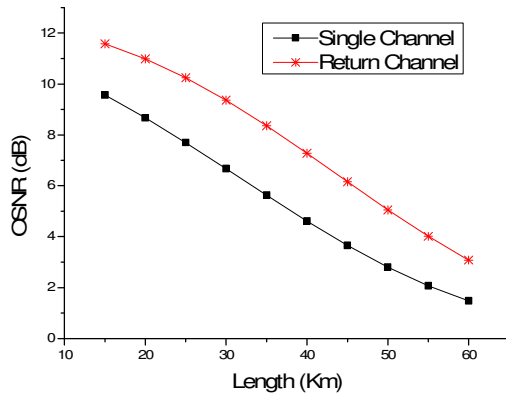


Figure 9 – OSNR vs. SMF length for the single channel setup and the setup with return channel

V. CONCLUSION

Sensors based on optical fibers and specially those based on FBGs and LPGs provide low cost and reliable solutions to measure environmental parameters. Many of the existing solutions consider compact devices and are not suited for remote sensing or are focused on distributed sensing [6]. Remote sensing using large spectrum sources (as is the case of sensors based on FBGs and LPGs) demands optical amplification for the sensor signal to reach the interrogation system with enough quality to be measured with good accuracy.

This work shows the potential of Raman amplification to solve these challenges and presents a numerical model capable of describing the Raman amplification and reproducing the spectrum of a remote LPG sensor with good accuracy around the resonance wavelength.

We also apply this model to study the signal amplification via Raman scattering in a hybrid sensor capable of measuring the environmental refractive index. It was shown that there is a linear relation between the power ratio of the central wavelength of each of the two FBGs however, amplification degrades seriously the sensitivity of the sensor due to the ASE noise and the Rayleigh Scattering. These drawbacks are solved by replacing the single fiber with two fibers: the first to connect the power source to the sensor head and the second responsible for the transmission of the sensor signal to the interrogation unit. This second fiber can be used either for the Raman amplification or to perform amplification in both fibers via a power splitter. This approach shows a sensitivity improvement due to the better OSNR levels of the optical signals.

ACKNOWLEDGMENT

The first author would like to acknowledge the “CAPES – Coordenação de Aperfeiçoamento de Pessoal de Nível Superior” and “FAPES – Fundação de Amparo a Pesquisa do Espírito Santo” for the support given to the work leading to this article.

REFERENCES

- [1] J. M. Lopez-Higuera, “Handbook of Optical Fibre Sensing Technology,” in *Plastics*, 2nd ed. vol. 3, J. Peters, Ed. New York: McGraw-Hill, 1964, pp. 15–64.
- [2] Coelho, T. V. N., Pontes, M. J., Cani, S. P., “Melhora da Precisão por Conservação de Energia do Modelo Analítico para Amplificadores Raman.” *Proc. MOMAG*, (2010).
- [3] M. N. Islam, “Raman Amplifier For Telecommunications 1. Physical Principles,” *Springer Series in Optical Sciences*, EUA, 2004.
- [4] Bromage, J., “Raman Amplification for Fiber Communication System.” *Journal of Lightwave Technology* 22, 79-93 (2004).
- [5] Jesus, C., Caldas, P., Frazão, O., Santos, J. L., Jorge, P. A. S. and Baptista, J. M., “Simultaneous Measurement of Refractive Index and Temperature Using a Hybrid Fiber Bragg Grating/Long-Period Fiber Grating Configurations.” *Fiber and Integrated Optics* 28, 440-449 (2009).
- [6] Xu, Z., Liu, D., Liu, H., Sun, Q., Sun, Z., Zhang, X. and Wang, W., “Design of Distributed Raman Temperature Sensing System Based on Single-mode Optical Fiber.” *Front. Optoelectron.* 2, 215-218 (2009).